PCCP

Accepted Manuscript

ROYAL SOCIETY OF CHEMISTRY

www.rsc.org/pccp

Journal Name

RSCPublishing

ARTICLE

Effects of fixed pattern noise on single molecule localization microscopy

Cite this: DOI: 10.1039/x0xx00000x

F. Long, S. Q. Zeng, and Z. L. Huang*[ab]

Received 00th January 2012,
Accepted 00th January 2012

DOI: 10.1039/x0xx00000x

www.rsc.org/

The newly developed scientific complementary metal oxide semiconductor (sCMOS) cameras are capable of realizing fast single molecule localization microscopy without sacrificing field-of-view, benefiting from their readout speed which is significantly higher than that of conventional charge-coupled device (CCD) cameras. However, the poor image uniformity (suffered from fixed pattern noise, FPN) is a major obstruction for a widespread use of sCMOS cameras in single molecule localization microscopy. Here we present a quantitative investigation on the effects of FPN on single molecule localization microscopy via localization precision and localization bias. We found that FPN leads to almost no effect on localization precision, but introduces a certain amount of localization bias. However, for a commercial Hamamatsu Flash 4.0 sCMOS camera, such localization bias is usually < 2 nm and thus can be neglected for most localization microscopy experiments. This study addresses the FPN concern which worries researchers, and thus will promote the application of sCMOS cameras in single molecule localization microscopy.

1. Introduction

Single molecule localization microscopy (often abbreviated as localization microscopy) compensates for the resolution drawback of conventional fluorescence microscopy, and offers diffraction-unlimited spatial resolution down to nanometres.[1-3] Due to its prominent imaging capability and relative simple setup, this new technique has attracted intensive attention from various research fields.[4-6] Localization microscopy essentially relies on the detection and localization of weak fluorescence emission from single molecules; therefore, choosing an appropriate low-light detector is key and also necessary to guarantee sufficient visibility for single molecules.[7, 8] Unsurprisingly, electron multiplying charge-coupled device (EMCCD) cameras, which are famous for the high sensitivity (quantified by wavelength-dependent quantum efficiency) and low read noise, have become the most widely used detector in localization microscopy.[7, 8]

On the other hand, as pointed out by the pioneers in the field of brain imaging[9, 10], the possibility of studying large volumes of tissue at the ultrastructural level will present a true revolution in studying important neurobiological problems that are not yet fully overcome by current imaging techniques. However, after taking a careful investigation on the technological challenges that remain, we realized that with the development of better fluorescent probes[11, 12], the demand of studying large volumes of tissue at the ultrastructural level cannot be met from the existing localization microscopy which utilizes EMCCD cameras as the detector, since the low readout speed of commercial EMCCD cameras (~10 MHz) cannot provide satisfactory acquisition speed and/or field of view without sacrificing spatial resolution.

In recent years, several groups have been investigating the potentials of utilizing new low-light cameras in single molecule imaging.[13-17] In particular, we proposed[14] that the scientific complementary metal oxide semiconductor (sCMOS) cameras, which usually offer high sensitivity and low read noise at extreme high readout speed (up to 560 MHz[18]), may provide a promising solution for realizing fast localization microscopy with extended field of view. We demonstrated the applicability of a commercial sCMOS camera (Hamamatsu Flash 2.8) in localization microscopy by imaging actin bundles labelled with d2EosFP.[13] Further, we developed an experimental methodology to quantitatively comparing the performance of low-light cameras. With this methodology we found that a newly launched sCMOS camera (Hamamatsu Flash 4.0) can present better imaging performance than a popular EMCCD

[a]Britton Chance Center for Biomedical Photonics, Wuhan National Laboratory for Optoelectronics-Huazhong University of Science and Technology, Wuhan 430074, China E-mail: leo@mail.hust.edu.cn
[b]Key Laboratory for Biomedical Photonics, Department of Biomedical Engineering,, Huazhong University of Science and Technology, Wuhan 430074, China

camera (Andor iXon 897) in the signal range of 15-20000 photon/pixel (which is more than enough for typical localization microscopy), and that the excess noise in the EMCCD cameras effectively halves the quantum efficiency.[14] However, there are still several technical issues[19] to be addressed before putting sCMOS cameras to practical use in localization microscopy.

One of the most important issues to be addressed is the image nonuniformity, which suffers from fixed pattern noise (FPN).[19] FPN originates from the mismatches between pixel and column readouts across camera sensor, and is defined as any noise components that survive frame averaging with uniform illumination.[20] For CCD-based cameras with single chip-level readout, the FPN is introduced by the difference between pixels, which is originated from the mismatches of pixel size and imperfections during the sensor manufacturing process (thus called pixel FPN, pFPN); while for CMOS-based cameras which have hundreds of column-level readouts in parallel, an additional FPN (called column FPN, cFPN) is introduced by offset and gain difference between column readouts.[21] Since the pixels across a camera are spatially uncorrelated, the pFPN behaves in a visible uniformity. However, the cFPN is column correlated, and results in visible stripes in an image even when the cFPN magnitude is lower than that of the pFPN.[22] Therefore, CMOS-based cameras typically suffer from the additional cFPN, and often provide poorer image uniformity than CCD-based cameras. Not surprisingly, FPN is often considered as a major disadvantage obstructing the use of CMOS-based cameras in microscopy.[23]

Recently, Bewersdorf et al [17] developed an sCMOS-specific algorithm which accounts for the pixel-dependent camera noises (including read noise and FPN), and achieved unbiased, precise localization at the theoretical limit. However, the influence of FPN in sCMOS on the single molecule localization has not been investigated quantitatively and systematically. Moreover, in localization microscopy, a final super-resolution image is reconstructed from molecule location information rather than raw single molecule images. Therefore, the impacts of FPN on localization microscopy may not be as severe as those on conventional microscopy. Nevertheless, a quantitative investigation on the effects of FPN on single molecule localization will surely provide useful information and/or build confidence for utilizing sCMOS cameras in localization microscopy.

In this paper, we present a systematic investigation on the effects of FPN on single molecule localization via bias (accuracy) and standard deviation (precision) of the locations by comparison to the true position. The magnitude of FPN was adapted from experimental measurements upon commercial sCMOS and EMCCD cameras, and the signal intensities were from representative chemical dye Alexa Fluor 647 and fluorescent protein mEos2.

2. Methods

2.1 Characterizing camera fixed pattern noise

Fixed pattern noise (FPN) can be calculated from image frames at different uniform illumination intensities. The optical setup for FPN measurement is the same as that of photon transfer curve (PTC), which was reported in detail in our previous paper.[13] Here, a set of 100 image frames was acquired continuously under certain uniform illumination intensity to estimate the camera FPN in corresponding signal intensity.

We note that FPN is composed of offset FPN and gain FPN. Offset FPN (also called dark signal non-uniformity, DSNU) is independent of signal, while gain FPN (also called photo response nonuniformity, PRNU) increases with signal intensity.[24] Therefore, in the data analysis method, we modified the method reported by Abbas El Gamal[21] to separate the offset and gain FPN. The specific analysis process is described below.

Measuring offset FPN

The offset FPN can be estimated from image frames acquired without incident light. First, the random noise components are reduced by averaging K image frames ($S_{i,j,k}$) with the following equation:

$$\mathrm{Offset}_{i,j} = \frac{1}{K}\sum_{k=1}^{K} S_{i,j,k} \quad (1)$$

where i and j are the pixel coordinates, k is the frame number, and K represents the total number of image frames.

The mean value of $\mathrm{Offset}_{i,j}$ across the pixel array is subtracted to leave only the offset FPN component $R_{i,j}^{Offset}$.

$$R_{i,j}^{Offset} = \mathrm{Offset}_{i,j} - \overline{\mathrm{Offset}} \quad (2)$$

For CMOS-based cameras, the offset cFPN originates from offset mismatches between column readouts. Therefore, the offset cFPN component, R_j^{col}, can be estimated by averaging the $R_{i,j}^{Offset}$ values of pixels (i,j) which share the same column output.[21] Here we assume that averaged offset pFPN component is zeros due to the fact that the offset pFPN for different pixels is uncorrelated random variables.

$$R_j^{col} = \frac{1}{N}\sum_{i=1}^{N} R_{i,j}^{Offset} \quad (3)$$

The offset pFPN component, $R_{i,j}^{pixel}$, is obtained by subtracting the offset cFPN component from the $R_{i,j}^{Offset}$ [21]:

$$R_{i,j}^{pixel} = R_{i,j}^{Offset} - R_j^{col} \quad (4)$$

Then the variances of offset cFPN and offset pFPN components, σ_{col}^2 and σ_{pixel}^2, are calculated respectively[21]:

$$\sigma_{col}^2 = \frac{1}{M\text{-}1}\sum_{j=1}^{M} (R_j^{col})^2 \quad (5)$$

$$\sigma^2_{pixel} = \frac{1}{M(N-1)} \sum_{i=1}^{N} \sum_{j=1}^{M} (R_j^{pixel})^2 \quad (6)$$

where M and N represent the number of columns and rows in the pixel array, respectively.

However, for CCD-based cameras which have no column FPN, the variances of offset pFPN component can be calculated directly as shown:

$$\sigma^2_{pixel} = \frac{1}{M(N-1)} \sum_{i=1}^{N} \sum_{j=1}^{M} (R_{i,j}^{Offset})^2 \quad (7)$$

Finally, for CMOS-based and CCD-based cameras, the offset pFPN and offset cFPN are characterized as the standard deviation of each offset FPN components as:

$$\text{offset pixel FPN} = \sqrt{\sigma^2_{pixel}} \quad (8)$$

$$\text{offset column FPN} = \sqrt{\sigma^2_{col}} \quad (9)$$

Measuring gain FPN

The gain FPN of CMOS-based and CCD-based cameras under certain signal intensity can be calculated with similar procedures as offset FPN using image frames under corresponding uniform illumination intensity. However, the offset FPN components should be removed when averaging image frames to reduce random noise:

$$\overline{S_{i,j}} = \frac{1}{K} \sum_{k=1}^{K} S_{i,j,k} - Offset_{i,j} \quad (10)$$

Then the averaged value of $\overline{S_{i,j}}$ across the pixel array, $\bar{s}$, is subtracted to leave only the gain FPN component $R_{i,j}^{Gain}$,

$$R_{i,j}^{Gain} = \overline{S_{i,j}} - \bar{s} \quad (11)$$

Finally, the variances of gain pFPN and gain cFPN components under illumination intensity of $\bar{s}$ can be calculated with similar data processing steps as those of offset FPN (Eqs. 3-7) using $R_{i,j}^{Gain}$ to place $R_{i,j}^{Offset}$. And the gain pFPN and gain cFPN are characterized as the standard deviation of each gain FPN components. Note that the gain FPN magnitude is usually expressed as the ratio of the gain FPN value to the illumination intensity.

2.2 Single molecule image simulation

The output signal (or image) from a low-light camera reflects not only the incident light intensity, but also the imperfections and noises of the camera itself. We model the output signal of pixel (i, j) from a low-light camera as:

$$y_{i,j} = x_{i,j} + SN_{i,j} + FPN_{i,j}^{gain} + FPN_{i,j}^{offset} + RN_{i,j} \quad (12)$$

where $x_{i,j}$ is the total signal from single molecule fluorescence signal (with two-dimensional Gaussian profile) and photon background; $SN_{i,j}$ denotes the shot noise, and $(x_{i,j}+SN_{i,j})$ follows Poisson distribution with mean value of $x_{i,j}$; $RN_{i,j}$ denotes the read noise of the camera and has Gaussian distribution with mean value of zero; $FPN_{i,j}^{gain}$ and $FPN_{i,j}^{offset}$ are the gain and offset FPN of the camera, respectively. Note that this model does not include dark noise, since it is negligible for low-light cameras.

Because gain FPN increases with the collected signal intensity, Eq. 12 can be simplified as:

$$y_{i,j} = F_{i,j} \times (x_{i,j} + SN_{i,j}) + RN_{i,j} + FPN_{i,j}^{offset} \quad (13)$$

where $F_{i,j}$ represents the gain FPN factor and can be used to characterize the two-dimension spatial profile of gain FPN. Combined the section of **Measuring gain FPN**, $F_{i,j}$ equals to the ratio of $\overline{S_{i,j}}$ to $\bar{s}$.

For CCD-based cameras, FPN is mainly introduced by pixel-to-pixel difference. The gain FPN factor can be express as[21]

$$F_{i,j} = X_{i,j} \quad (14)$$

where $X_{i,j}$ is the gain pFPN factor of pixel (i,j).

However, CMOS-based cameras suffer from additional column FPN. The pixel and column FPN originate from different sources and have no correlation with each other, thus the gain FPN factor of CMOS-based cameras can be expressed with the following form[21]:

$$F_{i,j} = X_{i,j} + Y_j \quad (15)$$

where $X_{i,j}$ is the gain pFPN factor of pixel (i, j), and Y_j is the gain cFPN factor of the pixels located in the j_{th} column. Because there is no correlation between pixels or columns in a camera, the $X_{i,j}$ and Y_j can be modeled as Gaussian distributed random variables with mean value of 1. Related with the previous section of **Measuring gain FPN**, the standard deviations of $X_{i,j}$ and Y_j represent the magnitude of gain pFPN and gain cFPN, respectively. Therefore in this paper, gain pFPN and gain cFPN factors ($X_{i,j}$ and Y_j respectively) were sampled from a Gaussian distribution with mean value of 1 and standard deviation of the predetermined FPN magnitude in the single molecule image simulation.

2.3 Single molecule data analysis

In localization microscopy, the performance of single molecule localization directly influences the reconstructed final super-resolution image. Here, we use localization bias and localization precision, which are defined from their statistical properties (see below), to quantify the effects of FPN on single molecule localization. Note that this kind of defination was also used in a recent review by Deschout et al.[25]

Fluorescence images acquired from a stationary single molecule located in (x_0, y_0) were used in the evaluation. It is well-known that the center positions of the molecule can be obtained by Gaussian fitting to the fluorescence images, and the obtained positions usually spread across a two-dimensional

plane. Therefore, the localization error can be characterized from the statistics of the center position distribution. To better quantify such localization error, we use localization precision to represent the width of the center position distribution, and localization bias to represent the drift of the center position distribution from the true position of the molecule (see Fig. 1).

The localization precision is obtained from averaging the standard deviation of the center position distribution in x and y dimensions:

$$\sigma = (\sigma_x + \sigma_y)/2 \quad (16)$$

The localization bias is calculated by the distance from the distribution mean to the true position of the molecule:

$$u = \sqrt{(u_x - x_0)^2 + (u_y - y_0)^2} \quad (17)$$

where σ_x and σ_y are the standard deviations of the center position distribution in x and y dimensions, respectively; and u_x and u_y are the mean values of the distribution in x and y dimensions, respectively.

The molecule positions are determined by fitting fluorescence images to a two-dimension Gaussian function using maximum likelihood estimator. It has been proved that this estimator achieves unbiased localization with precision closest to the Cramér-Rao Lower Bound.[26-28]

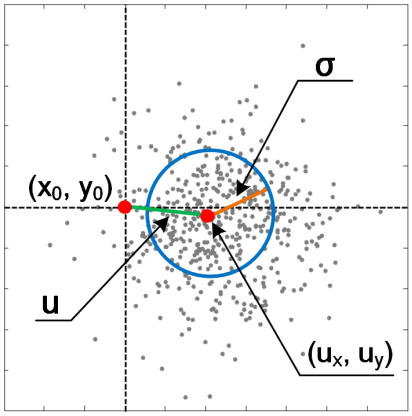

Fig. 1. Illustration of localization precision and bias. The stationary single molecule has a true position in (x_0, y_0), but is found via Gaussian fitting to have a 2D position distribution which has mean value of (u_x, u_y) and standard deviation of σ.

2.4 Implementation

To test the effects of FPN on single molecule localization, according to Eq. 14 or Eq. 15, a total number of 100 different FPN patterns were generated randomly for each FPN magnitude. For each pattern, a set of 3000 images with 13 × 13 pixels were generated using Eq. 13, where (1) the molecules were located in the center of the images; (2) the PSF was modeled with a Gaussian function whose standard deviation was set to be 130 nm; and (3) the pixel size at sample plane was set to be 130 nm (meaning that the point spread function occupies 5 × 5 pixels), unless specified otherwise. Because the offset FPN is lower than the gain FPN by one order of magnitude in the typical signal range in localization microscopy (see Section 2.1 for details), in the simulation we ignored the offset FPN to simplify Eq. 13.

The localization precision and bias were obtained by averaging all the values from 100 different patterns. All of the data generation and analysis were performed using MATLAB (MathWorks) on the same desktop computer.

3. Results and Discussion

3.1 FPN in different cameras

According to the FPN measurement method described in **Methods**, we measured the FPN in different signal intensities of a commercial high-end sCMOS camera--Hamamatsu Flash 4.0, and a representative EMCCD camera--Andor iXon 897 with EM Gain of 1 and 120, respectively. The results are shown in Fig. 2. It was found that in the typical signal range of localization microscopy (50-2000 photon/pixel[14]), for the Flash 4.0 sCMOS and the iXon 897 EMCCD with EM Gain of 120, the gain FPN is higher than the offset FPN by an order of magnitude (Fig. 2). It is consistent with reports that the offset FPN can be significantly reduced by correlated double sampling.[20, 23, 24] Therefore in this paper, we simply ignore the offset FPN, and concentrate on the effects of gain FPN on single molecule localization. In the following, the fixed pattern noise represents the gain FPN, unless otherwise specified.

In the high signal intensity range (> 3000 photon/pixel), for the Flash 4.0 sCMOS camera and the iXon 897 EMCCD camera with EM Gain of 1, the pFPN increases almost proportionally with signal intensity. Specifically, for the Flash 4.0 sCMOS camera, the magnitude of cFPN and pFPN (corresponding to the slopes of the experimental curves) is 0.12% and 0.6%, respectively, and the cFPN is 3~5 times smaller than the pFPN. For the iXon 897 EMCCD camera with EM Gain 1, the magnitude of pFPN is 0.25%, indicating that the pixel sensitivity uniformity of the EMCCD camera is better than that of the sCMOS camera. However, in the low signal intensity range (< 2000 photon/pixel), the pFPN in the Flash 4.0 sCMOS camera is significantly smaller than that in the iXon 897 EMCCD camera with EM Gain of 1, and larger (up to 5 times) than that in the same EMCCD camera working at EM gain of 120. Note that the signal intensity for the iXon 897 EMCCD camera with EM Gain of 120 is < 2000 photon/pixel.[14]

In addition, regarding the noise components of the Flash 4.0 sCMOS camera, it is worthy to note that: (1) it is the signal shot noise rather than the FPN which contributes dominantly to the total noise in the signal range of 4~18000 photons/pixel (see Fig. 4a in the paper by Long et al [14]), (2) the FPN is equal to or smaller than the read noise when signal is smaller than 300 photon/pixel (See Fig. 3a and Fig. 4a in the paper by Long et al [14]), (3) most of the cFPN magnitude are < 0.5% signal in the typical signal range of localization microscopy (50~2000 photon/pixel (see the red rectangle in Fig. 2), and (4) the pFPN of the Flash 4.0 sCMOS camera is larger than that of the iXon

897 EMCCD camera with EM Gain of 120 in a wide signal range.

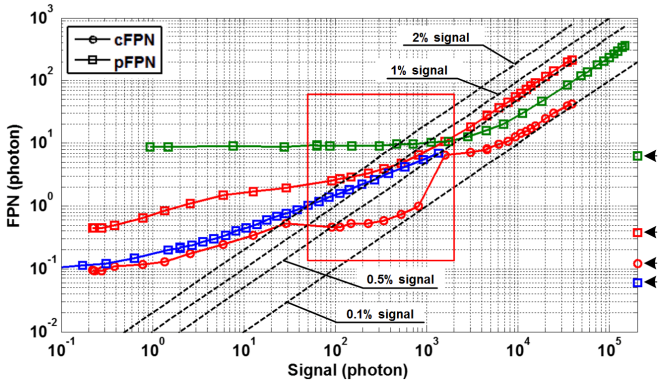

Fig. 2. Offset and gain FPN for the Flash 4.0 sCMOS camera (red), the iXon 897 EMCCD camera with EM Gain of 1 (green) and 120 (blue). The connected data points present the dependence of gain FPN on signal intensity, while the isolated data points in the right vertical axis show the constant offset FPN. Note that the red rectangle highlights the typical signal range in localization microscopy.

3.2 The effects of FPN on conventional microscopy

To evaluate the effects of FPN on conventional microscopy, we used the models in **Methods** and generated simulated FPN factor map, where the pFPN magnitude was set to be 1% (a medium value selected from Fig. 2) and the cFPN magnitude was set to range from 0 to the full value of the pFPN magnitude. Note that FPN correction techniques are usually used in CMOS-based cameras to guarantee that cFPN is smaller than pFPN.[22, 23] The results are shown in Fig. 3.

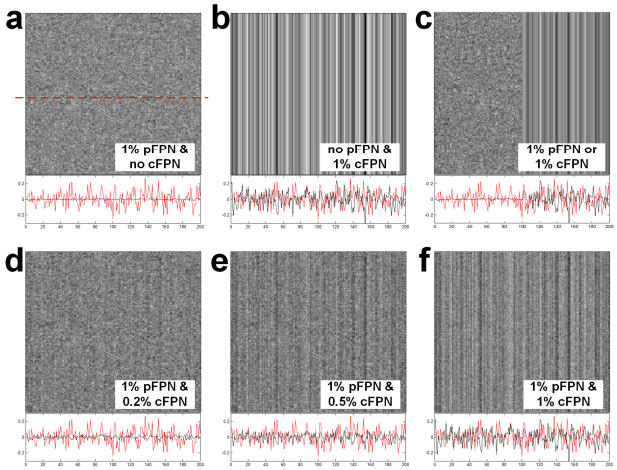

Fig. 3. The effects of cFPN on image uniformity. The magnitude of the pFPN and cFPN factors is shown in the right corner of the corresponding images. The averaged cFPN factors (black curves) are shown in the bottom of each images, along with the fluctuation of the 1% pFPN factors (red curves) which was obtained from the red dotted line in a.

It is clear that cFPN is the major source of the vertical stripe structures (Figs. 3a-c). And, the vertical stripe structures become visible with increasing cFPN magnitude (Figs. 3d-f), and cause seriously distortion to the image uniformity when the cFPN magnitude equals to the pFPN (1% in our case, see Fig. 3f). These simulated results confirm the previous finding by Snoeij et al that the spatial structure of cFPN has stronger perceptual effect to the human visual system even when the magnitude of cFPN is significantly lower than that of pFPN.[22]

3.3 The effects of FPN on single molecule localization for a representative signal intensity

We evaluated the effects of FPN on single molecule localization for a representative fluorescent probe Alexa Fluor 647. We considered three different noise scenarios: (1) random noises only; (2) random noises and 1% pFPN; (3) random noises and 1% cFPN. For the random noises, here we considered only signal shot noise, background shot noise and read noise. Specifically, the signal and background intensities were set to be 3000 photon/molecule and 80 photon/pixel, respectively. [29] The read noise was set to be 1 e-, which is close to the measured value from the Flash 4.0 sCMOS camera under studied. The generation and analysis of single molecule images were described in **Methods**. The results are shown in Fig. 4.

As can be seen from Figs. 4a-b, the values of the localization precision in all of the three scenarios are almost the same: 0.0265 pixel (Scenario 1), 0.0265±0.0001 pixel (Scenario 2), and 0.0265±0.0001 pixel (Scenario 3). However, the localization bias is < 0.001 pixel when there are only random noises (Scenario 1), and increases noticeably after adding 1% pFPN (0.0052±0.0029 pixel) or 1% cFPN (0.0059±0.0048 pixel) (see Figs. 4c-d). These findings show that FPN, regardless of whether it is pFPN or cFPN, introduces negligible influence on localization precision, but causes noticeable effect on localization bias.

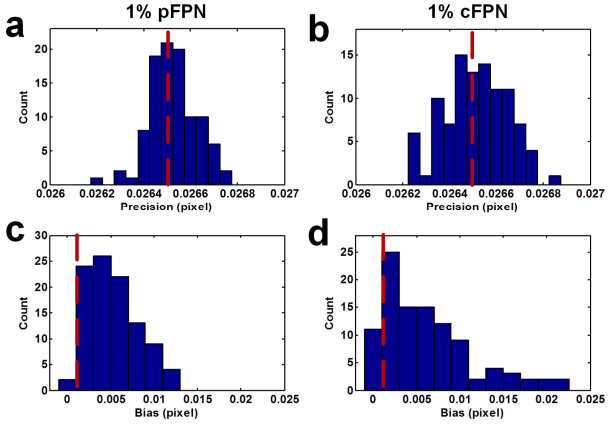

Fig. 4. The effects of FPN on single molecule localization. The histograms of single molecule localization precision (a, b) and bias (c, d). In (a, c) the pFPN magnitude was set to be 1%, and in (b, d) the cFPN magnitude was set to be 1%. The red lines present the localization precision or bias values under no FPN. In the simulation, the signal and background intensities were set to be 3000 photon/molecule and 80 photon/pixel, respectively, the pixel size was 130 nm, and the standard deviation of Gaussian PSF was 130 nm. The localization precision and bias for each data count were calculated from 3000 simulated image frames, and the total number of data counts was 100, corresponding to 100 different FPN patterns.

3.4 General effects of FPN on localization microscopy

Localization microscopy utilizes reconstructed images rather than the original ones to reveal details of biological structures. Therefore, the effects of FPN on localization microscopy can be mainly observed from the information of molecule location, including the center positions of each molecule and the corresponding localization error. In this sense, it is beneficial to have a closer look at the reasons why FPN introduces almost no effects on localization precision, but leads to noticeable effect to localization bias.

According to Webb et al[30], when conventional CCD-based cameras are used to capture the fluorescence emission from a stationary single molecule, the fluctuation of time-dependent noises (here called random noises, including mainly signal shot noise, background shot noise and read noise) will essentially present if such image acquisition is repeated. Therefore, the center positions of the molecule obtained by further single molecule localization will present a 2D distribution whose statistical mean is unbiased to the true position due to the stochastic characteristic of the random noises (see Section 2.3, Scenario 1).

However, FPN also exists in CCD-based cameras due to intrinsic pixel-to-pixel difference.[20] This kind of FPN (called pFPN) will cause noticeable effects on localization bias, although pFPN plays almost no influence to the localization precision (see Section 2.3, Scenario 2). Similar effects can be observed for a proposed camera which has cFPN and no pFPN (see Section 2.3, Scenario 3). Therefore, since CMOS-based cameras suffer from both cFPN and pFPN, greater localization bias can be expected, while localization precision could still be neglected.

From the discussions shown above, we illustrate the general effects of FPN on localization microscopy (see Fig. 5). In an ideal camera without FPN, repeated detection and localization of the fluorescence emission from a stationary molecule (Fig. 5a) will present a position distribution (Fig. 5d) which is centered in the fluorescence image. The standard deviation of such distribution, usually defined as localization precision (σ), reflects the effects of time-dependent noise components on single molecule localization. However, if FPN (appeared as a time-unchanged patterns, see Fig. 5b) is also presented in the camera, the corresponding fluorescence image will be distorted (Fig. 5c), leading to a noticeable shift in the center of the position distribution (Fig. 5e).

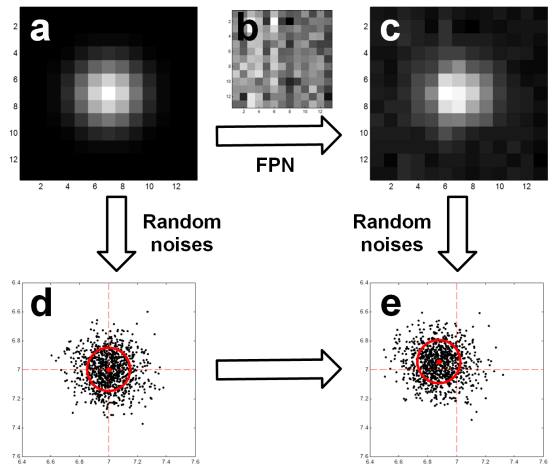

Fig. 5. Illustration for the effects of FPN on single molecule localization. (a) A representative ideal fluorescence image from a stationary single molecule (located in the image center). (b) A FPN factor map. (c) Distorted fluorescence image from the stationary molecule. (d-e) Positions distribution of the stationary molecule from repeated single molecule detection and localization without (d) and with (e) the effects of FPN.

3.5 The effects of FPN on single molecule localization under different signal and background intensities

Here we use three scenarios to represent different types of cameras, including (1) Ideal cameras without FPN, (2) CCD-based cameras with only pFPN, and (3) CMOS-based cameras with both pFPN and cFPN. After considering the FPN magnitude of real cameras (Fig. 2), we set the pFPN magnitude of the CCD-based cameras to be 1%, and the pFPN and cFPN magnitude of the CMOS-based cameras to be 1% and 0.5%, respectively. Image generation and data analysis were described in **Methods**. The results are shown in Fig. 6. The effects of other FPN magnitude on single molecule localization will be studied in Section 2.6.

We firstly have a close look into the results from the same background intensity and varied signal intensities (Figs. 6a-b). We found that the values of localization precision decrease with brighter signal intensities for all three scenarios, and that FPN leads to almost no effects to the localization precision. However, FPN noticeably affects the localization bias. More precisely, the mean localization bias in **Camera Scenario 2** (CCD-based cameras with only 1% pFPN) is 5-10 times larger than that in **Camera Scenario 1** (Ideal camera without FPN), and is > 9 times larger than the standard deviation of the localization bias in **Camera Scenario 1**. Moreover, for **Camera Scenario 3** (CMOS-based cameras with 1% pFPN and 0.5% cFPN), the mean and standard deviation of localization bias have an increase of ~20% and ~30%, respectively, to those in **Camera Scenario 2**. However, the mean localization bias is still within the standard deviation of the localization bias in **Camera Scenario 2**. These conclusions also apply to situations with a low background, for example, 5 photon/pixel, which is common in TIRF illumination. Note that the FPN varies significantly from individual cameras and/or different pixel regions inside a camera, thus we did not investigate the local

behaviours of several special FPN patterns on single molecule localization. However, the local behaviours distribution can be revealed by the error bars in Fig. 6. We also investigated the case of varied background intensities and a fixed signal intensity, which is either 3000 photon/molecule to mimic chemical dye Alexa Fluor 647 (Figs. 6c-d), or 750 photon/molecule to mimic fluorescent protein mEos2 (Fig. 6e-f). Similar to the previous case, we found that FPN leads to almost no effects on the localization precision, but noticeably increase on the localization bias.

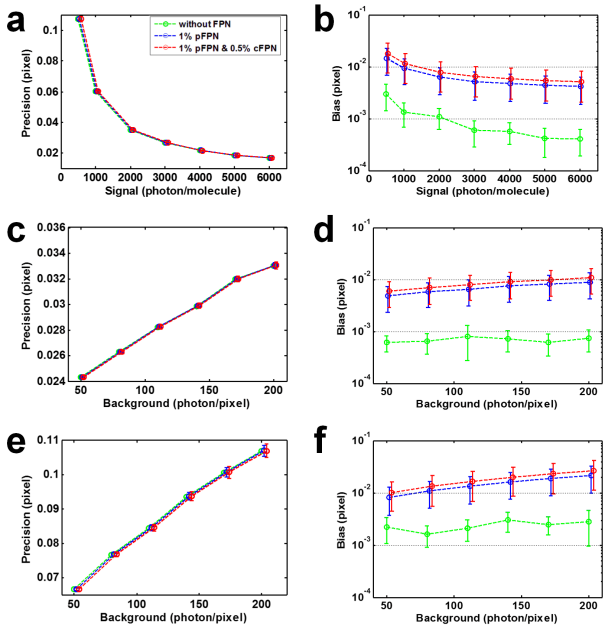

Fig. 6. The effects of FPN on single molecule localization under different signal and background intensities. The background intensity was set to be 80 photon/pixel (a, b), and the signal intensity was set to be 3000 photon/molecule (c, d) and 750 photon/molecule (e, f), respectively. The green, blue and red lines are for ideal, CCD-based and CMOS-based cameras, respectively. The FPN magnitudes are shown in (a). Each of the data points in (a-f) was averaged from 100 different FPN patterns. For each FPN pattern, the localization precision and bias were calculated from 3000 simulated image frames. The pixel size was 130 nm, and the standard deviation of Gaussian PSF was 130 nm. The standard deviations of the localization precision and bias from the 100 different FPN patterns are indicated by the error bars.

Taking all the above findings together, we realize that the difference between **Camera Scenario 2** (CCD-based cameras with 1% pFPN) and **Camera Scenario 3** (CMOS-based cameras with 1% pFPN and 0.5% cFPN) is actually very difficult to observe, since there is almost no difference in the localization precision, while the difference in localization bias is within the standard deviation (thus is not statistically significant). Therefore, for the Flash 4.0 sCMOS camera where the cFPN is much smaller than the pFPN (especially in the signal intensity range of 80~1000 photon/pixel, see Fig. 6b in the paper by Long et al [14]), the effects from cFPN are hard to observe, while the effects from pFPN should be paid more attention (see Section 2.6 for further discussions).

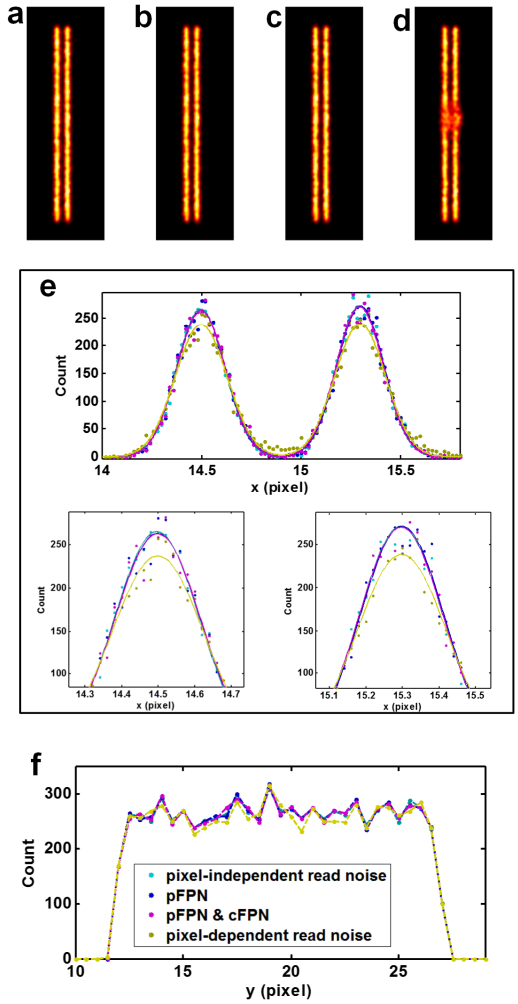

Fig. 7. The local effects of FPN and high read noise on single molecule localization under different noise scenarios. (a-d) The reconstructed images for **Camera Scenarios 4-7** (from left to right), respectively. (e-f) The positions distribution in x (vertical to the lines) and y (horizontal to the lines) dimensions, respectively. Note that in (e) the solid lines are the Gaussian fits using the data points, and the details of the peaks are enlarged and shown below.

We further estimated the local behavior of the precision and biases introduced by FPN. We firstly added Poisson noise and pixel-independent read noise (1.3 e-) to a noise-free image (34 × 43 pixels) with two parallel lines to generate simulated images for a hypothetical camera with only Poisson noise and read noise (**Camera Scenario 4**). The following parameters were used in the simulation: Signal = 200 photon/molecule; Background = 5 photon/pixel; Pixel size = 130 nm; Gaussian PSF with the standard deviation of 130 nm; Line length = 15 pixel, Line width = infinitesimal; Line separation = 0.8 pixel; and no more than 1 molecule is randomly distributed in the images. Then additional noises were added into **Camera Scenario 4**, including 1% pFPN (**Camera Scenario 5**), 1% pFPN and 0.5% cFPN (**Camera Scenario 6**). Using the same parameters, we also generated simulated images for a special scenario (**Camera Scenario 7**) which has Poisson noise, high pixel-dependent read noise (26 e-) in pixel (16, 19) (in the right side of the lines), and 1.3 e- in other pixels. The reconstructed

images are shown in Fig. 7. We found that the shapes (Figs. 7a-c) and positions (Figs. 7e-f) of the reconstructed lines are almost kept the same for **Camera Scenario 4-6**, indicating that the local impact of the 1% pFPN and/or 0.5% cFPN are too small to be visualized. However, for **Camera Scenario 7**, we observed a good amount of distortion in the reconstructed structures close to the pixel with high read noise (Fig. 7d-f). Actually, a recent paper by Bewersdorf et al reported that the pixel-dependent noises (including read noise and FPN) of sCMOS cameras introduced localization artifacts.[17] The results in this study (in particular, Fig. 7) suggest that those localization artifacts are possibly originated from high pixel-dependent read noise, rather than FPN. Of course, more investigations may be required to further confirm the hypothesis, but is beyond the scope of this study.

3.6 Minimizing localization bias

Sometimes it is desired to characterize nanometer scale structures with both high localization precision and accuracy.[31, 32] The localization precision can be improved by repeating the measurement until photobleaching, which is equivalent to increase the collected signal.[30] Unfortunately, the localization bias cannot be improved through this approach, because the FPN is fixed between different image frames. Therefore, it is necessary to find out an effective approach for minimizing the localization bias. For this purpose, it is of primary importance to pay attention to the relationship among localization bias, the FPN magnitude (determined by the camera used) and the pixelation (corresponding to different pixel sizes at sample). Similar to the previous sections, here we considered single molecule imaging of either Alexa Flour 647 or mEos2, and kept consistent signal and background intensities with our experiments.

The dependence of localization bias on FPN magnitude

The simulation and data analysis were described in **Methods**. A total number of 100 FPN patterns were used. For each FPN pattern, the FPN magnitude was adjusted by increasing the FPN factor $F_{i,j}$ proportionally. For the CMOS-based camera scenario, the cFPN magnitude was set to be half of the pFPN magnitude. The results are shown in Fig. 8.

We found that for a certain FPN pattern, the dependence of localization bias on FPN magnitude is almost linear, although the slope for such dependence varies with different FPN patterns (see the error bars in Fig. 8). Moreover, the localization bias for the CMOS-based camera scenario is ~20% higher than that of the CCD-based camera scenario, which suffers from the additional column FPN.

After considering the measured FPN of the Flash 4.0 sCMOS camera and the iXon 897 EMCCD camera with EM Gain 120 (Fig. 2), we found that the iXon 897 EMCCD can achieve lower localization bias than the Flash 4.0 sCMOS camera due to smaller pFPN. That is to say, more efforts are required to reduce the FPN in the Flash 4.0 sCMOS camera.

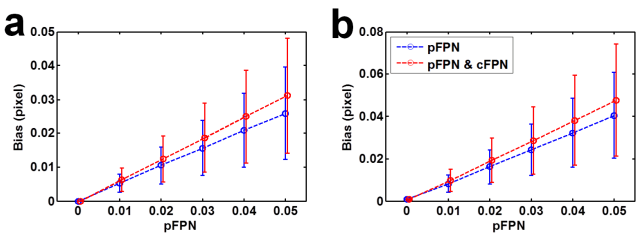

Fig. 8. The dependence of localization bias on FPN magnitudes. (a) The signal and background intensities were set to be 3000 photon/molecule and 80 photon/pixel, respectively, for mimicking Alexa Fluor 647. (b) The signal and background intensities were 750 photon/molecule and 50 photon/pixel, respectively, for mimicking mEos2. The data in blue are for the CCD-based camera scenario, and the data in red are for the CMOS-based camera scenario. Each data point was averaged from 100 different FPN patterns. For each FPN pattern, the localization precision and bias were calculated from 3000 simulated image frames. The pixel size was 130 nm, and the standard deviation of Gaussian PSF was 130 nm. The standard deviations of the bias from the 100 different FPN patterns are indicated by the error bars.

The dependence of localization bias on pixelation

We investigate the dependence of localization bias on pixelation (that is, different pixel size at sample) under two FPN magnitudes: (1) 1% pFPN only, and (2) 1% pFPN and 0.5% cFPN. For both high (Fig. 9a) and low (Fig. 9b) signal intensity cases, we observed that the absolute value of localization bias (in nanometer unit) actually increases with greater pixel size, while adding 0.5% cFPN to the existing 1% pFPN leads to ~20% increase in the localization bias.

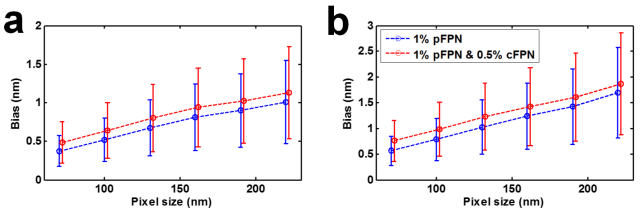

Fig. 9. The dependence of localization bias on the pixel size at sample. (a) The signal intensity was set to be 3000 photon/molecule, and the background was set to be 4734 photon/um^2 (equals to 80 photon/pixel when the pixel size is 130 nm), to mimic Alexa Fluor 647. (b) The signal was set to be 750 photon/molecule, the background was set to be 2959 photon/um^2 (equals to 50 photon/pixel when the pixel size is 130 nm), to mimic mEos2. The data in blue are for the CCD-based camera scenario, while the data in red are for the CMOS-based camera scenario. Each data point was averaged from 100 different FPN patterns. For each FPN pattern, the localization precision and bias were calculated from 3000 frame simulation images. The standard deviation of Gaussian PSF was 130 nm. The standard deviations of bias from the 100 different FPN patterns are indicated by the error bars.

3.7 Minimizing localization bias for localization microscopic experiments

From previous discussions, we observed that FPN leads to almost no effects on localization precision, but noticeable effects on localization bias. Furthermore, we found that localization bias is proportional to the FPN magnitude and the pixel size at sample (see Figs. 8 and 9).

According to our simulated results, if it is desirable to obtain a localization bias smaller than 1 nm, we should pay attention not only to the time-dependent noises (including mainly signal shot noise, and background shot noise) and

pixelation noise, but also to the FPN. For a rough guidance, we should carefully choose a bright fluorescent probes (the signal intensity should be > 1000 photon/molecule), minimize fluorescence background (the background intensity should be < 50 photon/pixel), optimize microscope magnification (the pixel size at sample is preferable to be < 100 nm), and select a camera with small FPN (the pFPN factor should be < 1%, and the cFPN factor is at least half of the pFPN factor).

We estimated the localization precision and bias for the commercial iXon 897 EMCCD and Flash 4.0 sCMOS cameras. The results are summarized in Table 1. Interestingly, the localization precision from the Flash 4.0 sCMOS camera is found to be higher (that is, smaller values) than that from the iXon 897 EMCCD camera, which is mainly due to the excess noise in the EMCCD camera. Meanwhile, the EMCCD camera exhibits better performance (smaller values) in the localization bias than the sCMOS camera, which is surely resulted from the higher FPN magnitude of the latter camera.

Furthermore, we observed that the values of localization precision are > 5 times larger than the corresponding localization bias. This finding indicates that the FPN of commercial cameras had a noticeable but not statistically significant effect on localization microscopy. And, when the signal is higher than 1000 photon/molecule, the localization bias of commercial cameras is usually < 2 nm and thus can be neglected for most localization microscopy experiments (see Fig. 6 and Table 1). Of course, in applications which required extremely high localization precision and localization bias, it is still beneficial to carry out more accurate FPN calibration.

Table 1. Estimated localization precision and bias for two commercial cameras

Signal	Camera[c]	Precision (nm)	Bias (nm)
High[a]	iXon 897 EMCCD	4.94	0.52 ± 0.27
	Flash 4.0 sCMOS	4.03	0.57 ± 0.31
Low[b]	iXon 897 EMCCD	12.48	1.13 ± 0.65
	Flash 4.0 sCMOS	10.27	1.69 ± 0.91

Notes: (a) Signal = 3000 photon/molecule, background = 80 photon/pixel, pixel size = 130 nm. (b) Signal = 750 photon/molecule, background = 50 photon/pixel, pixel size = 130 nm. (c) The quantum efficiency is set to be 0.95 for the iXon 897 EMCCD camera, and 0.72 for the Flash 4.0 sCMOS camera, respectively. The EM gain of the EMCCD camera was set to be 120. The excess noise was included into the calculation for the EMCCD camera. The pFPN and cFPN magnitude for different signal levels were taken from measurements (Fig. 2). Specifically, the FPN are as follows: (1) High signal case: $pFPN_{EMCCD} = 0.75\%$, $pFPN_{sCMOS} = 0.80\%$; $cFPN_{EMCCD} = 0$, $cFPN_{sCMOS} = 0.1\%$; (2) Low signal case: $pFPN_{EMCCD} = 1.1\%$, $pFPN_{sCMOS} = 1.5\%$; $cFPN_{EMCCD} = 0$, $cFPN_{sCMOS} = 0.2\%$.

Finally, we note that the impacts of FPN found in this study (< 2 nm) seem to be less obvious than those reported by Steven Chu et al (5-6 nm) [31]. The difference may be attributed to the different imaging models. In this study, we aim to investigate only the effects of FPN on single molecule localization, and thus employ a simple model: simulated images without experimental errors (laser intensity stability, mechanical stability, optical aberration, etc), and single color. In Chu's paper, a more complex imaging model is used: two-color localization, complicated experimental control. Therefore, comparing to the larger (experimental) values observed in Chu's paper, our finding possibly reflect a lower (theoretical) limit in the impacts of FPN.

4. Conclusions

Basing on simulation, we systematically investigated the effects of fixed pattern noise (FPN) on single molecule localization. We found that the FPN (including pixel and column FPN) introduces negligible effects on the localization precision, but noticeable effects on the localization bias (up to several nanometres). We further observed that, for commercial iXon 897 EMCCD and Flash 4.0 sCMOS cameras where pixel FPN is typically larger than column FPN, the effects of column FPN on single molecule localization are hard to observe, while pixel FPN had a noticeable but not statistically significant effect on single molecule localization. However, if it is desirable to obtain a localization bias smaller than 1 nm, we should have a good selection not only on the signal and background intensities and the pixel size at sample, but also on the FPN magnitude. Moreover, we suggest that for applying commercial sCMOS cameras in localization microscopy, it is of great beneficial to pay more attention to compensate the effects from hot pixels (high read noise), rather than FPN.

Acknowledgements

This work was supported by National Basic Research Program of China (Grant No. 2011CB910401), the Science Fund for Creative Research Group of China (Grant No. 61121004), the National Natural Science Foundation of China (Grant No. 91332103), and the Program for New Century Excellent Talents in University of China (Grant No. NCET-10-0407). We appreciate Mr. Tadashi Maruno, Mr. Eiji Toda and Dr. Keith Bennett from Hamamatsu Photonics for technical support on the Flash 4.0 sCMOS camera and helpful discussions.

Notes and references

1. E. Betzig, G. H. Patterson, R. Sougrat, O. W. Lindwasser, S. Olenych, J. S. Bonifacino, M. W. Davidson, J. Lippincott-Schwartz and H. F. Hess, *Science*, 2006, **313**, 1642-1645.
2. M. J. Rust, M. Bates and X. Zhuang, *Nat. Methods*, 2006, **3**, 793-795.
3. S. T. Hess, T. P. Girirajan and M. D. Mason, *Biophys. J.*, 2006, **91**, 4258-4272.
4. A. Dani, B. Huang, J. Bergan, C. Dulac and X. W. Zhuang, *Neuron*, 2010, **68**, 843-856.
5. N. A. Frost, H. Shroff, H. H. Kong, E. Betzig and T. A. Blanpied, *Neuron*, 2010, **67**, 86-99.
6. K. Xu, G. S. Zhong and X. W. Zhuang, *Science*, 2013, **339**, 452-456.
7. T. J. Gould, V. V. Verkhusha and S. T. Hess, *Nat. Protoc.*, 2009, **4**, 291-308.
8. H. Shroff, H. White and E. Betzig, *Curr. Protoc. Cell Biol.*, 2008, **Chapter 4**, Unit 4.21.
9. J. DeFelipe, *Science*, 2010, **330**, 1198-1201.
10. J. W. Lichtman and W. Denk, *Science*, 2011, **334**, 618-623.
11. J. F. Lovell and G. Zheng, *JIOHS*, 2008, **1**, 45-61.

12. M. Zhu, G. Zhang, C. Li, Y. Li, M. P. Aldred and A. D. Q. LI, *JIOHS*, 2011, **4**, 395-408.
13. Z. L. Huang, H. Zhu, F. Long, H. Ma, L. Qin, Y. Liu, J. Ding, Z. Zhang, Q. Luo and S. Zeng, *Opt. Express*, 2011, **19**, 19156-19168.
14. F. Long, S. Zeng and Z. L. Huang, *Opt. Express*, 2012, **20**, 17741-17759.
15. S. Saurabh, S. Maji and M. P. Bruchez, *Opt. Express*, 2012, **20**, 7338-7349.
16. T. W. Quan, S. Q. Zeng and Z. L. Huang, *J. Biomed. Opt.*, 2010, **15**, 066005.
17. F. Huang, T. M. P. Hartwich, F. E. Rivera-Molina, Y. Lin, W. C. Duim, J. J. Long, P. D. Uchil, J. R. Myers, M. A. Baird, W. Mothes, M. W. Davidson, D. Toomre and J. Bewersdorf, *Nat. Methods*, 2013, **10**, 653-658.
18. B. Fowler, C. A. Liu, S. Mims, J. Balicki, W. Li, H. Do, J. Appelbaum and P. Vu, *Proc. SPIE*, 2010, **7536**, 753607-753612.
19. M. Baker, *Nat. Methods*, 2011, **8**, 1005-1009.
20. J. R. Janesick, *Photon transfer : DN [lambda]*, SPIE, Bellingham, Wash., 2007.
21. A. El Gamal, B. Fowler, H. Min and X. Q. Liu, *Proc. SPIE*, 1998, **3301**, 168-177.
22. M. F. Snoeij, A. J. P. Theuwissen, K. A. A. Makinwa and J. H. Huijsing, *IEEE J. Solid-St. Circulation*, 2006, **41**, 3007-3015.
23. M. Bigas, E. Cabruja, J. Forest and J. Salvi, *Microelectronics J.*, 2006, **37**, 433-451.
24. A. El Gamal and H. Eltoukhy, *IEEE Circuits and Devices Magazine*, 2005, **21**, 6-20.
25. H. Deschout, F. C. Zanacchi, M. Mlodzianoski, A. Diaspro, J. Bewersdorf, S. T. Hess and K. Braeckmans, *Nat Methods*, 2014, **11**, 253-266.
26. A. V. Abraham, S. Ram, J. Chao, E. S. Ward and R. J. Ober, *Opt. Express*, 2009, **17**, 23352-23373.
27. C. S. Smith, N. Joseph, B. Rieger and K. A. Lidke, *Nat. Methods*, 2010, **7**, 373-375.
28. T. W. Quan, P. C. Li, F. Long, S. Q. Zeng, Q. M. Luo, P. N. Hedde, G. U. Nienhaus and Z. L. Huang, *Opt. Express*, 2010, **18**, 11867-11876.
29. L. Zhu, W. Zhang, D. Elnatan and B. Huang, *Nat. Methods*, 2012, **9**, 721-723.
30. R. E. Thompson, D. R. Larson and W. W. Webb, *Biophys. J.*, 2002, **82**, 2775-2783.
31. A. Pertsinidis, Y. X. Zhang and S. Chu, *Nature*, 2010, **466**, 647-651.
32. A. Yildiz, J. N. Forkey, S. A. McKinney, T. Ha, Y. E. Goldman and P. R. Selvin, *Science*, 2003, **300**, 2061-2065.